

ARTICLE

Received 24 Apr 2014 | Accepted 29 Jul 2014 | Published 11 Sep 2014

DOI: 10.1038/ncomms5843

# Impermeable barrier films and protective coatings based on reduced graphene oxide

Y. Su<sup>1</sup>, V.G. Kravets<sup>1</sup>, S.L. Wong<sup>1</sup>, J. Waters<sup>2</sup>, A.K. Geim<sup>1</sup> & R.R. Nair<sup>1</sup>

Flexible barrier films preventing permeation of gases and moistures are important for many industries ranging from food to medical and from chemical to electronic. From this perspective, graphene has recently attracted particular interest because its defect-free monolayers are impermeable to all atoms and molecules. However, it has been proved to be challenging to develop large-area defectless graphene films suitable for industrial use. Here we report barrier properties of multilayer graphitic films made by gentle chemical reduction of graphene oxide laminates with hydroiodic and ascorbic acids. They are found to be highly impermeable to all gases, liquids and aggressive chemicals including, for example, hydrofluoric acid. The exceptional barrier properties are attributed to a high degree of graphitization of the laminates and little structural damage during reduction. This work indicates a close prospect of graphene-based flexible and inert barriers and protective coatings, which can be of interest for numerous applications.

<sup>1</sup>School of Physics and Astronomy, University of Manchester, Manchester M13 9PL, UK. <sup>2</sup>School of Earth, Atmospheric and Environmental Sciences, University of Manchester, Manchester M13 9PL, UK. Correspondence and requests for materials should be addressed to A.K.G. (email: geim@manchester.ac.uk) or to R.R.N. (email: rahul.raveendran-nair@manchester.ac.uk).

Membranes made from graphene and its chemical derivative called graphene oxide<sup>1–3</sup> (GO) show a range of unique barrier properties<sup>4–8</sup>. Defect-free monolayer graphene is impermeable to all gases and liquids<sup>4</sup> and, similar to graphite, shows high chemical and thermal stability with little toxicity. These characteristics are believed to provide graphene with a competitive edge over the existing barrier materials<sup>9</sup>. Unfortunately, prospects of using graphene as a protective coating are hampered by difficulties of growing large-area defect-free films. For example, it is shown that graphene films grown by chemical vapour deposition (CVD) possess many defects and grain boundaries and do not protect copper against oxidation but, to the contrary, speed up its corrosion<sup>10</sup>. A potential solution to this problem is the use of graphene-based multilayers<sup>11–13</sup>. In this respect, GO is particularly attractive because multilayer films can be produced easily and relatively cheaply by depositing GO solutions on various substrates by spraying, and dip- or rod-coating, and so on. The resulting GO laminates are shown to exhibit highly unusual permeation properties<sup>5–8</sup>. In the dry state, they are impermeable even for helium but, under humid conditions, provide no barrier for water vapour<sup>5</sup>. If immersed in water, the laminates act as molecular sieves allowing transport of small ions and blocking large ones<sup>6</sup>. Although such unique and contrasting properties may be useful for certain applications, many others need flexible barrier films with little oxygen and moisture permeation. The required rates are typically  $<0.1$  g of water per  $\text{m}^2$  per day and down to  $10^{-6}$   $\text{g m}^{-2}$  per day in the case of flexible organic electronics<sup>9,14</sup>. Achieving these ultra-low rates for the case of flexible coatings is extremely challenging<sup>14</sup>. For comparison, the commonly used metallized polyethylene terephthalate (PET) films (40–50 nm Al on 12  $\mu\text{m}$  PET further covered with a 75- $\mu\text{m}$  low-density polyethylene) allow water permeation rates of  $\sim 0.5$   $\text{g m}^{-2}$  per day<sup>15</sup>. In this report, we explore the possibility of enhancing the barrier properties of GO laminates by using the fact that molecular permeation through them occurs along interlayer capillaries of  $\approx 10$  Å in width<sup>5,6</sup>. This distance can be decreased using chemical reduction and approaches 3.4 Å in bulk graphite. If no significant structural damage is induced by the process, it is reasonable to expect much improved barrier properties for reduced GO laminates.

Considerable efforts have recently been made to utilize multilayer graphene-based films (thermally reduced GO (T-RGO)<sup>11,12</sup>, CVD graphene<sup>13</sup> and graphene-based composites<sup>9</sup>) as ultra-barriers for organic electronics and as oxidation-resistant and anticorrosion coatings<sup>9,16–22</sup>. However, T-RGO membranes are extremely fragile and contain many structural defects, which results in notable water permeation<sup>5,9</sup>. A high density of defects in CVD graphene also limits its possible uses<sup>9,10</sup>. Similarly, GO-polymer composites have so far exhibited gas permeability too high to consider them for realistic applications<sup>9</sup>. To increase the quality of GO-based coatings, it is essential to decrease the number of defects formed during the reduction process<sup>23–28</sup> (see Supplementary Fig. 1 and Supplementary Note 1). Recent studies show that the use of hydroiodic (HI) acid as a reducing agent results in RGO's quality being much higher than that provided by other reduction techniques, in terms of electrical and mechanical properties<sup>25,27,29</sup>. The HI reduction leaves fewer structural defects and little deformation so that the mechanical strength increases, becoming even higher than that for initial GO laminates that are known to be already exceptionally strong<sup>1</sup>. Another interesting reducing agent is ascorbic acid, that is, vitamin C (VC)<sup>26,28</sup>. It shows not only good reducing characteristics but stands out as environment friendly and nontoxic, which may be a critical factor in certain applications. Both reducing agents are believed to convert most of the functional groups attached to graphene into

$\text{H}_2\text{O}$ , which results in little structural damage of graphene sheets during reduction<sup>25–29</sup>.

In this contribution, we report permeation properties of GO laminates reduced using HI and VC. Both free-standing membranes and thin coatings on various substrates have been examined. Such RGO films are found to provide high-quality barriers that block all gases and liquids. In particular, if GO laminates are reduced in HI, no permeation of hydrogen and moisture could be detected for films as thin as 30 nm, which remain optically transparent. The films thicker than 100 nm exhibit no detectable permeation with respect to all tested gases and liquids. Furthermore, the RGO laminates are found to be impermeable to strong chemicals and salt solutions. These exceptional properties open a practical route towards graphene-based chemical-resistant and anticorrosion paints and coatings.

## Results

### Permeation properties of free-standing RGO membranes.

Figure 1a shows examples of water permeation measurements through GO and RGO membranes. In agreement with the previous reports<sup>5,6</sup>, non-reduced membranes were found to be impermeable to all gases, except for  $\text{H}_2\text{O}$  that evaporated with little resistance. After thermal reduction, the same membranes exhibited  $\sim 10$  times slower water loss but became fragile. Permeation rates for three different T-RGO samples were measured and varied by a factor of 2. In contrast, GO membranes reduced in VC (VC-RGO) exhibited a decrease by 5 orders of magnitude in water transmission rates with respect to pristine GO laminates (Fig. 1b) with little ( $<20\%$ ) variation for six studied samples. HI-reduced GO membranes (HI-RGO; more than 10 samples) provided even a better barrier such that water permeation became undetectable within our best accuracy of  $\approx 0.1$  mg per week. This sets an upper limit for moisture permeation through HI-RGO films as  $10^{-2}$   $\text{g m}^{-2}$  per day and  $\sim 10^{-11}$   $\text{mm g s}^{-1} \text{bar}^{-1} \text{cm}^{-2}$  (see Fig. 1b). Despite being only the limit for our detection technique, this value is already nearly two orders of magnitude lower than water transparency for the industry-standard barrier films (aluminized PET)<sup>30</sup>. Note that the HI-RGO membranes were impermeable under both liquid and vapour conditions, with the former studied by using the same container but turned upside down so that liquid water was in direct contact with the membranes (See methods). As a crosscheck, we also performed measurements for several

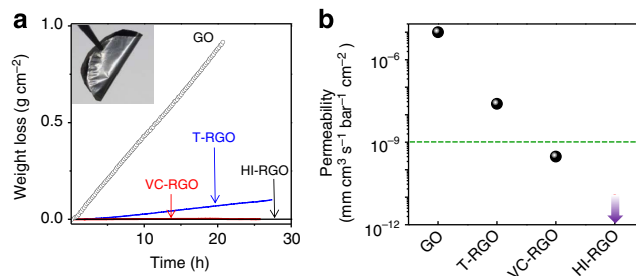


**Figure 1 | Water permeation through free-standing multilayer graphene membranes.**

(a) Water loss from a container sealed with GO and RGO membranes with a diameter of  $\approx 2$  cm (thickness  $d \approx 0.5$   $\mu\text{m}$ ). For GO, the loss is the same as through an open aperture and limited by water evaporation. Inset: photo of an HI-RGO membrane (diameter  $\approx 2$  cm).

(b) Permeability of various RGO membranes with respect to moisture. The arrow indicates our detection limit. Permeability of pristine GO is taken from ref. 5. Green line: water permeability for the industrial-standard barrier films estimated using data of ref. 30 for 30 nm Al on PET.

organic solvents such as acetone, methanol, ethanol and propanol and found no detectable permeation.

**Permeation properties of RGO-coated PET.** It is more practical to use RGO not as free-standing membranes but as thin coatings on top of other materials. To evaluate barrier properties of such coatings, we have employed standard PET films (12- $\mu\text{m}$  thick) as a support. Figure 2 shows an optical photo of the PET film covered with 30 nm of HI-RGO (See methods and Supplementary Fig. 2). Despite the much smaller thickness  $d$  than in the case of the RGO membranes discussed above, such optically transparent flexible barrier films show no detectable permeation of either hydrogen or water (Fig. 2b). Again, the moisture barrier is at least two orders of magnitude better than that provided by Al films of similar thickness. However, 30-nm-thick HI-RGO was still found to be slightly permeable to He, which can be attributed to occasional microscopic pinholes or structural defects in thin laminates that are made of randomly stacked graphene crystallites<sup>5–8</sup>. It requires HI-RGO films thicker than 100 nm to block He permeation completely, beyond the leak detection test that is the most sensitive method to check for potential leaks in high vacuum equipment (upper inset of Fig. 2a). To assess the possible influence of humidity on He permeation<sup>5</sup>, we tested HI-RGO films in the presence of saturated water vapour and found no difference with respect to dry conditions. Furthermore, we carried out water permeation experiments at elevated temperatures of up to 45 °C and 100% humidity and found that the moisture barrier did not degrade. We have also tested a VC-RGO coating on PET and did not observe any significant difference with respect to HI-RGO. Importantly, chemically reduced GO exhibits strong adhesion to PET and, despite sub-micrometre thickness, withstands folding, stretching and moderate scratching, which allows normal handling procedures similar to Al-coated PET (Supplementary Fig. 3 and Supplementary Note 2).

**Anticorrosion and chemical protection properties of RGO.** The discussed superior barrier properties of HI/VC-RGO laminates suggest their possible use as anticorrosion and chemical-resistant coatings<sup>13,17,21</sup>. To evaluate barrier properties with respect to salts and acids, we have used the measurement set-up described in ref. 6. Briefly, two compartments of a U-shaped container were separated by a free-standing membrane and then filled, one with pure water and the other with a salt solution (concentrations

varied from sub-Molar to full saturation). Salt diffusion was monitored by measuring its concentration in the pure water compartment by using ion chromatography and gravimetric analysis<sup>6</sup>. Figure 3a illustrates our results for the case of 1 M NaCl. Cl ions permeate rapidly through non-reduced GO membranes, in agreement with the earlier report<sup>6</sup>. However, within our experimental accuracy<sup>6</sup>, no salt permeation could be detected through either HI- or VC-RGO membranes.

To further illustrate anticorrosion properties of our graphitic laminates, we have tested their protection against HF, one of the most corrosive acids. The upper insets of Fig. 3a show the effect of HF on oxidized Si wafers (300 nm of SiO<sub>2</sub>), which were protected with 0.5- $\mu\text{m}$ -thick films of GO and VC-RGO. A drop of concentrated HF was placed on top of the coatings and continuously maintained for several hours. Then the coating was peeled off to assess damages. As evident from Fig. 3a, HF permeated through the GO film, as expected<sup>6</sup>, and etched through the entire thickness of the SiO<sub>2</sub> layer. On the other hand, the RGO film fully protected the wafer against HF, and no sign of SiO<sub>2</sub> etching could be detected within our accuracy of better than 10 nm. Similar acid drop tests were carried out for RGO coatings on top of various metals, including Cu and Ni. The latter foils were exposed to nitric and hydrochloric acids in different concentrations (0.1–10 M) but no degradation of the surface could be observed after several days of exposure. Furthermore, VC-RGO-coated Ni and steel foils were immersed in saturated iron chloride and sodium chloride solutions for many days and, again, no degradation could be detected. Finally, we covered glass petri dishes with HI-RGO (bottom inset of Fig. 3a). This graphitic lining allowed the glassware to use HF.

Finally, we note that most substrates used in our work had smooth surfaces (PET, metal foils). However, we have also tried GO coating on materials with rough surfaces such as, for example, conventional bricks. Despite brick's highly porous structure, VC-RGO films exhibited excellent barrier properties, too (Supplementary Fig. 4 and Supplementary Note 3). Furthermore, adhesion of RGO films to metal surfaces is found to be weaker than to plastic ones. This makes the protective coatings of metals more prone to mechanical scratching and peeling off. To overcome this problem, we have mixed a GO solution with polyvinyl alcohol (PVA) and used the binary solution to make GO-PVA films in the same manner as described in the methods. The resulting dry composites contained  $30 \pm 10\%$  of PVA. After their chemical reduction, the coatings exhibited

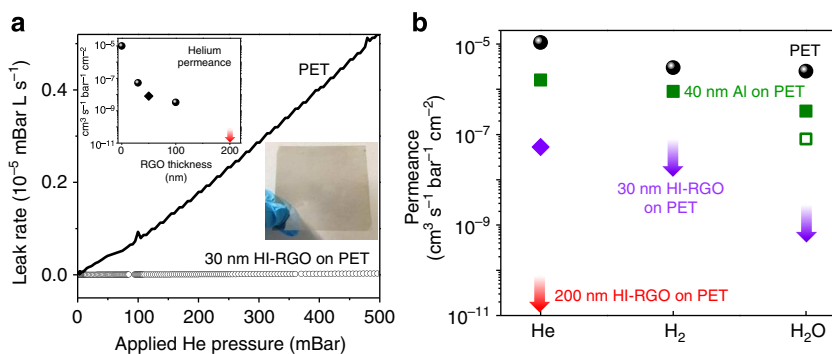


**Figure 2 | Permeation through RGO barrier coatings.** (a) He-leak measurements for a bare PET film (12  $\mu\text{m}$ ) and the same film coated with 30 nm of HI-RGO (normalized per  $\text{cm}^2$ ). The latter film is shown in the lower inset and exhibits an optical transparency of  $\approx 35\%$ . The transparency is reduced to 7% for 100-nm-thick RGO, and coatings thicker than 200 nm are opaque. Upper inset: He permeance (permeability divided by  $d$ ) as a function of HI-RGO thickness  $d$  (circles). The diamond symbol is for VC-RGO coating ( $d \approx 50$  nm). (b) Barrier properties of bare PET, HI-RGO on PET and aluminized PET with respect to He, H<sub>2</sub> and H<sub>2</sub>O. Bare PET films (circles) show permeance in agreement with literature values<sup>33</sup>. The solid green symbols are for a 40-nm-thick aluminium film on PET (our measurements) and the open symbol is for a 30-nm Al on PET (ref. 30). The violet and red arrows indicate our detection limits for 30 and 200 nm HI-RGO, respectively. Sample-to-sample variations for were less than 20%.

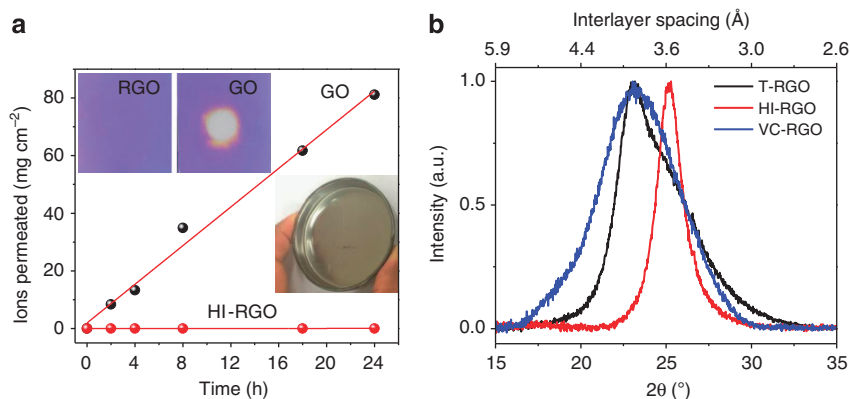


**Figure 3 | Chemical protection by RGO.** (a) Measurements of Cl-ion permeation through GO and HI-RGO membranes ( $d \approx 1 \mu\text{m}$ ). Upper inset: right and left photos ( $1 \text{ cm} \times 1 \text{ cm}$ ) show the effect of HF on oxidized Si wafers protected by GO and RGO, respectively.  $\text{SiO}_2$  is completely removed in the white centre region. Etching away of just 10 nm of  $\text{SiO}_2$  would be visible as changes in the interference colour, which are absent in the left image. Bottom inset: glass petri dish lined with HI-RGO ( $\approx 1\text{-}\mu\text{m}$  thick). (b) X-ray diffraction for thermally, HI- and VC-reduced GO membranes.

practically the same barrier properties as without PVA but with much improved adhesion and mechanical characteristics (Supplementary Fig. 5 and Supplementary Note 4).

## Discussion

To explain the observed barrier properties of RGO, we recall that permeation through non-reduced GO laminates occurs via a network of graphene capillaries filled with one or two monolayers of water<sup>5,6</sup>. The capillaries have a width varying from 0.7 to 1.3 nm, depending on humidity. After chemical or thermal reduction, these capillaries collapse, and the interlayer separation decreases to only  $\approx 0.36 \text{ nm}$ , which is close to the interlayer separation in graphite<sup>3</sup> (see Fig. 3b). This means that there is no space left for helium, water and other molecules to permeate between graphene sheets, and the only diffusion path remaining after the reduction is through structural defects. The crystallographic quality of reduced laminates can generally be judged by their X-ray diffraction peaks. Figure 3b shows that HI-RGO exhibits the sharpest peak indicating the highest degree of graphitization<sup>3,27</sup>. VC-RGO has a broader X-ray peak (Fig. 3b) but nonetheless shows barrier properties similar to those of HI-RGO. The only difference noticed between HI- and VC-RGO membranes was in their barrier properties with respect to moisture (see Fig. 1b). The remnant  $\text{H}_2\text{O}$  leakage for VC-RGO can be attributed to difficulties in reducing the membranes over their entire thickness by using VC that has larger and less mobile molecules than HI. However, approximately the same quality of graphitization for VC- and T-RGO films (Fig. 3b) indicates that factors other than the interlayer distance are important. We believe that the critical difference lies in the amount of structural defects formed during the reduction process. Indeed, it is known that during thermal reduction of GO, oxygen-containing functional groups are removed together with carbon atoms from graphene planes, which results in release of CO and  $\text{CO}_2$  gases<sup>3,23</sup>. They have to escape from the interior and, therefore, can delaminate and damage the layered structure (Supplementary Fig. 1 and Supplementary Note 1). On the contrary, chemical reduction by using HI and VC is much gentler, and most of the functional groups attached to graphene sheets react with the reducing agents releasing water instead of gases<sup>3,23</sup>, which can move along capillaries until they completely close behind<sup>5,6</sup>. As a result, our chemically reduced GO is less damaged and retains a better structural order (see Supplementary Note 1).

In conclusion, chemically reduced GO films (especially, using HI) exhibit exceptional barrier properties with respect to all tested gases, liquids, salts and acids, with no detectable permeation. Although our accuracy with respect to moisture is limited to  $\approx 10^{-2} \text{ g m}^{-2}$  per day, the known structural properties of HI-RGO allow us to expect that the moisture transmission should be similar to that for He and, therefore, would meet the stringiest industry requirements for flexible moisture barriers. The demonstrated films can be considered as thin graphitic linings, which can be produced on an industrial scale by solution processing. Taking into account that graphite is one of the most stable and chemically inert materials, this work opens a venue for many applications in which a barrier against moisture, oxygen and other gases and liquids is required and for the use in chemical and corrosion protection. The possibility to use the environment friendly reduction in ascorbic acid widens the scope of possible applications to sensitive areas including pharmaceuticals.

## Methods

**Preparation of GO and RGO membranes and coatings.** Graphite oxide was prepared by the Hummers method<sup>31</sup> and then dispersed in water by sonication, which resulted in stable GO solutions<sup>1-3</sup>. The size of individual GO flakes varied from  $\sim 0.2\text{--}20 \mu\text{m}$ , and we did not find any notable size dependence in the barrier properties described above. We used two types of RGO samples: free-standing membranes and supported thin films on various substrates. The free-standing membranes were fabricated by vacuum filtration as described in refs 5,6 and had thickness  $d$  from 0.5 to  $5 \mu\text{m}$ . The supported films were prepared by rod-coating<sup>32</sup> or spray-coating on top of  $12\text{-}\mu\text{m}$ -thick PET films, metal foils and oxidized silicon wafers. Thermal reduction was carried out at  $300^\circ\text{C}$  for 4 h in a hydrogen-argon mixture. HI reduction<sup>25,27</sup> was carried out by exposing GO films to the acid vapour at  $90^\circ\text{C}$ . The exposure time varied from 5 to 30 min, depending on  $d$ . Then, samples were repeatedly rinsed with ethanol to remove residual HI. For VC reduction<sup>26,28</sup>, GO films were immersed in water solution of VC ( $30 \text{ g l}^{-1}$ ) for 1 h at  $90^\circ\text{C}$ .

**Optical and AFM characterization of HI-RGO on PET.** To characterize RGO films on PET, we have used scanning electron microscopy, atomic force microscopy (AFM) and optical absorption spectroscopy. Supplementary Fig. 2 shows an absorption spectrum for a  $30\text{-nm}$ -thick film of HI-RGO. For the visible spectrum the transmittance varies from  $\approx 30$  to  $40\%$ . The thickness of RGO coatings was measured using a Veeco Dimension 3100 AFM in the tapping mode under ambient conditions. The inset of Supplementary Fig. 2 shows a representative AFM image for a  $30\text{-nm}$ -thick HI-RGO on PET.

**Permeability measurements.** Permeation properties of the various RGO films were measured using several techniques that were described in detail previously<sup>5,6</sup>. In brief, for vapour permeation measurements, free-standing membranes and RGO-on-PET films were glued to a Cu foil with an opening of  $2\text{-cm}$  diameter. The foil was clamped between two nitrile rubber O-rings sealing a metal



container<sup>5</sup>. Permeability was measured by monitoring the weight loss of the container that was filled with water and other liquids inside a glovebox<sup>5</sup>. In gas permeation experiments<sup>5</sup>, GO-on-PET films were placed between two standard rubber gaskets and pressurized from one side to up to 1 bar. Gas permeation was monitored on the opposite (vacuum) side by using mass spectrometry. We used INFICON UL200 that allowed the detection of helium and hydrogen.

**Evaluating permeability from weight loss experiments.** Permeability  $P$  was calculated from our weight loss measurements as  $P = Q \times d/A \times \Delta P$ , where  $Q$  is the weight loss rate,  $d$  the thickness of a membrane,  $A$  its area and  $\Delta P$  the differential pressure of water vapour across the membrane. Moisture permeation experiments were carried out in a glove box with a negligible water vapour (<0.5 p.p.m.) so that  $\Delta P$  was the partial pressure of water vapour at room temperature, that is,  $\sim 2,300$  Pa.

## References

- Zhu, Y. *et al.* Graphene and graphene oxide: synthesis, properties, and applications. *Adv. Mater.* **22**, 3906–3924 (2010).
- Loh, K. P., Bao, Q., Eda, G. & Chhowalla, M. Graphene oxide as a chemically tunable platform for optical applications. *Nat. Chem.* **2**, 1015–1024 (2010).
- Pei, S. & Cheng, H.-M. The reduction of graphene oxide. *Carbon* **50**, 3210–3228 (2012).
- Bunch, J. S. *et al.* Impermeable atomic membranes from graphene sheets. *Nano Lett.* **8**, 2458–2462 (2008).
- Nair, R. R., Wu, H. A., Jayaram, P. N., Grigorieva, I. V. & Geim, A. K. Unimpeded permeation of water through helium-leak-tight graphene-based membranes. *Science* **335**, 442–444 (2012).
- Joshi, R. K. *et al.* Precise and Ultrafast molecular sieving through graphene oxide membranes. *Science* **343**, 752–754 (2014).
- Kim, H. W. *et al.* Selective gas transport through few-layered graphene and graphene oxide membranes. *Science* **342**, 91–95 (2013).
- Li, H. *et al.* Ultrathin molecular sieving graphene oxide membranes for selective hydrogen separation. *Science* **342**, 95–98 (2013).
- Yoo, B. M., Shin, H. J., Yoon, H. W. & Park, H. B. Graphene and graphene oxide and their uses in barrier polymers. *J. Appl. Polym. Sci.* **131**, 39628 (2014).
- Schrivver, M. *et al.* Graphene as a long-term metal oxidation barrier: worse than nothing. *ACS Nano* **7**, 5763–5768 (2013).
- Kang, D. *et al.* Oxidation resistance of iron and copper foils coated with reduced graphene oxide multilayers. *ACS Nano* **6**, 7763–7769 (2012).
- Yamaguchi, H. *et al.* Reduced graphene oxide thin films as ultrabarrriers for organic electronics. *Adv. Energy Mater.* **4**, 1300986 (2014).
- Prasai, D., Tuberquia, J. C., Harl, R. R., Jennings, G. K. & Bolotin, K. I. Graphene: corrosion-inhibiting coating. *ACS Nano* **6**, 1102–1108 (2012).
- Lewis, J. Material challenge for flexible organic devices. *Mater. Today* **9**, 38–45 (2006).
- Mueller, K., Schoenweitz, C. & Langowski, H. C. Thin laminate films for barrier packaging application—influence of down gauging and substrate surface properties on the permeation properties. *Packag. Technol. Sci.* **25**, 137–148 (2012).
- Huang, H.-D. *et al.* High barrier graphene oxide nanosheet/poly(vinyl alcohol) nanocomposite films. *J. Membrane Sci.* **409–410**, 156–163 (2012).
- Kirkland, N. T., Schiller, T., Medhekar, N. & Birbilis, N. Exploring graphene as a corrosion protection barrier. *Corros. Sci.* **56**, 1–4 (2012).
- Yang, J. *et al.* Thermal reduced graphene based poly(ethylene vinyl alcohol) nanocomposites: enhanced mechanical properties, gas barrier, water resistance, and thermal stability. *Ind. Eng. Chem. Res.* **52**, 16745–16754 (2013).
- Yang, Y. H., Bolling, L., Priolo, M. A. & Grunlan, J. C. Super gas barrier and selectivity of graphene oxide-polymer multilayer thin films. *Adv. Mater.* **25**, 503–508 (2013).
- Tseng, I. H., Liao, Y.-F., Chiang, J.-C. & Tsai, M.-H. Transparent polyimide/graphene oxide nanocomposite with improved moisture barrier property. *Mater. Chem. Phys.* **136**, 247–253 (2012).
- Nilsson, L. *et al.* Graphene coatings: probing the limits of the one atom thick protection layer. *ACS Nano* **6**, 10258–10266 (2012).
- Guo, F. *et al.* Graphene-based environmental barriers. *Environ. Sci. Tech.* **46**, 7717–7724 (2012).
- Chua, C. K. & Pumera, M. Chemical reduction of graphene oxide: a synthetic chemistry viewpoint. *Chem. Soc. Rev.* **43**, 291–312 (2014).
- Some, S. *et al.* High-quality reduced graphene oxide by a dual-function chemical reduction and healing process. *Sci. Rep.* **3**, 1929 (2013).
- Pei, S., Zhao, J., Du, J., Ren, W. & Cheng, H.-M. Direct reduction of graphene oxide films into highly conductive and flexible graphene films by hydrohalic acids. *Carbon* **48**, 4466–4474 (2010).
- Zhang, J. *et al.* Reduction of graphene oxide via L-ascorbic acid. *Chem. Commun.* **46**, 1112–1114 (2010).
- Moon, I. K., Lee, J., Ruoff, R. S. & Lee, H. Reduced graphene oxide by chemical graphitization. *Nat. Commun.* **1**, 73 (2010).
- Fernández-Merino, M. J. *et al.* Vitamin C is an ideal substitute for hydrazine in the reduction of graphene oxide suspensions. *J. Phys. Chem. C* **114**, 6426–6432 (2010).
- Su, Y., Du, J., Sun, D., Liu, C. & Cheng, H. Reduced graphene oxide with a highly restored  $\pi$ -conjugated structure for inkjet printing and its use in all-carbon transistors. *Nano Res.* **6**, 842–852 (2013).
- Garnier, G. r., Yrieix, B., Brechet, Y. & Flandin, L. Influence of structural feature of aluminum coatings on mechanical and water barrier properties of metallized PET films. *J. Appl. Polym. Sci.* **115**, 3110–3119 (2010).
- Hummers, W. S. & Offeman, R. E. Preparation of graphitic oxide. *J. Am. Chem. Soc.* **80**, 1339–1339 (1958).
- Wang, J. *et al.* Rod-coating: towards large-area fabrication of uniform reduced graphene oxide films for flexible touch screens. *Adv. Mater.* **24**, 2874–2878 (2012).
- Mercea, P. V. & Bârțan, M. The permeation of gases through a poly (ethylene terephthalate) membrane deposited with SiO<sub>2</sub>. *J. Membrane Sci.* **59**, 353–358 (1991).

## Acknowledgements

This work was supported by the Engineering and Physical Sciences Research Council (UK), European Research Council and the Royal Society. We thank R.K. Joshi for help. R.R.N also acknowledges the support by the Leverhulme Trust.

## Author contributions

R.R.N. and A.K.G. designed the project, and R.R.N. directed it with the help of Y.S. Y.S., V.G.K and S.L.W. performed the experiments and data analyses. J.W. conducted XRD. R.R.N. and A.K.G. wrote the manuscript. All authors contributed to discussions.

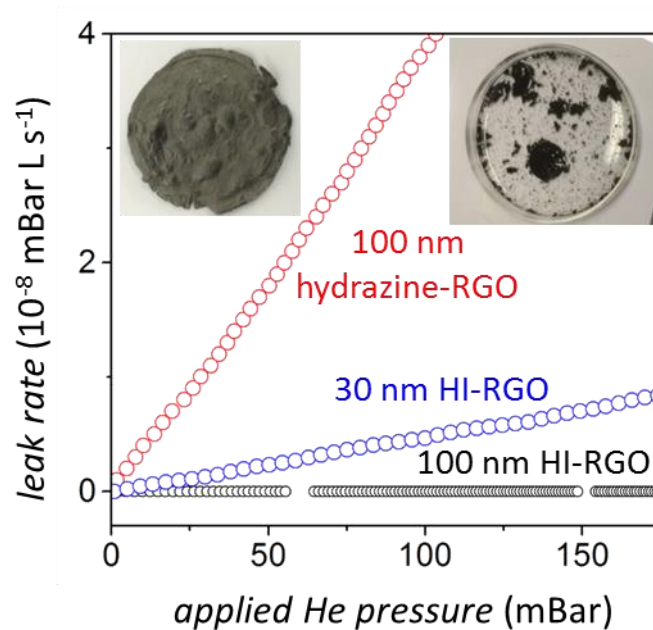
## Additional information

**Supplementary Information** accompanies this paper at <http://www.nature.com/naturecommunications>

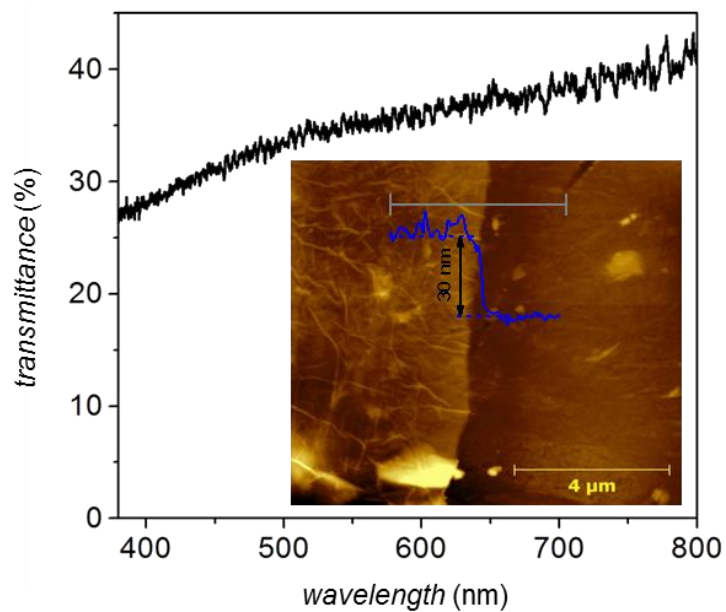
**Competing financial interests:** The authors declare no competing financial interests.

**Reprints and permission** information is available online at <http://npg.nature.com/reprintsandpermissions/>

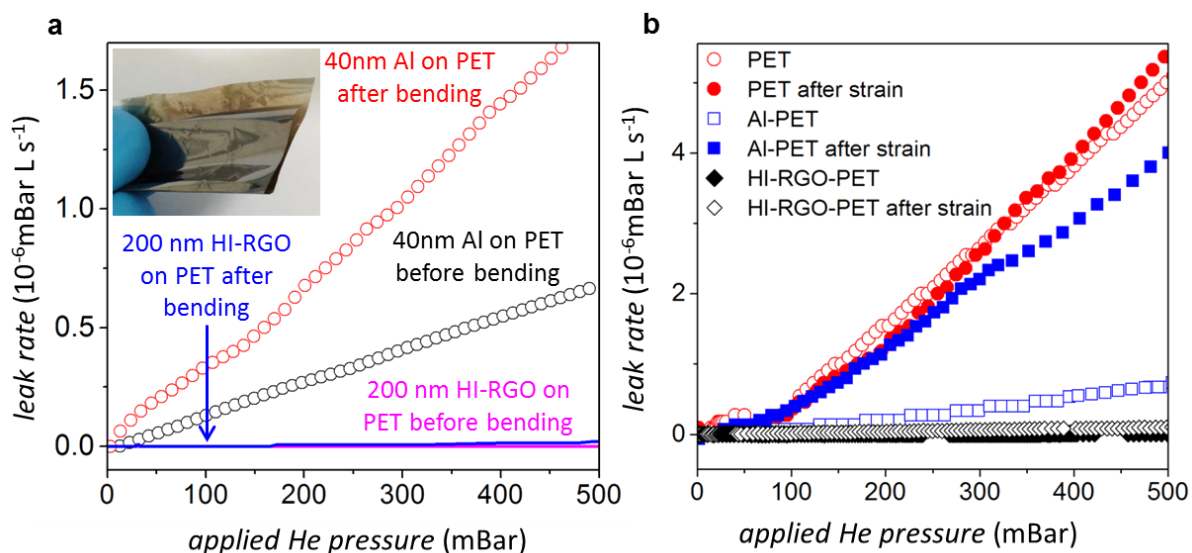
**How to cite this article:** Su, Y. *et al.* Impermeable barrier films and protective coatings based on reduced graphene oxide. *Nat. Commun.* **5**:4843 doi: 10.1038/ncomms5843 (2014).



**Supplementary Figure 1.** Comparison of He permeation through different chemically-reduced GO films. 30 nm HI-RGO is approximately 10 times less permeable than 100 nm GO reduced by hydrazine vapor. Both measurements are for coatings on 12  $\mu\text{m}$  PET and normalized per  $\text{cm}^2$ . The left inset shows a 2 cm diameter free standing GO membrane reduced by thermal reduction at 300  $^{\circ}\text{C}$  in a hydrogen-argon mixture for 4 hours. Right inset: GO membranes disintegrate during reduction in hydrazine solutions.



**Supplementary Figure 2.** Optical transmittance for a 30 nm thick HI-RGO on top of 12 μm thick PET with respect to bare PET. The inset shows an AFM image of the film near the boundary between bare PET and the RGO coating. Blue curve: Height profile along the gray line.

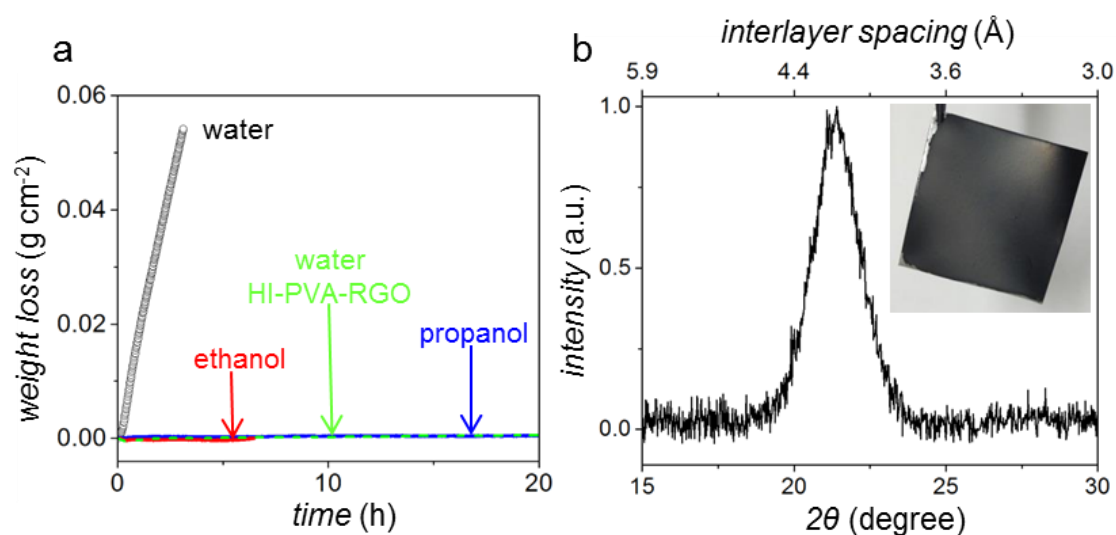


**Supplementary Figure 3.** Influence of mechanical deformation on barrier properties. **a** – He permeation through 40 nm Al and 200 nm HI-RGO (both on 12  $\mu$ m PET) before and after multiple folding. Inset: photograph of the tested HI-RGO. **b** – He permeation through bare PET, 40 nm thick Al on PET and <50 nm thick HI-RGO on PET before and after their straining. The strain was created by an argon pressure of 2 bar applied to one side of the membranes with vacuum on the other side.





**Supplementary Figure 4.** Photograph demonstrating water permeation through a brick (~20 cm long) with and without VC-RGO coating. Brick without the graphitic coating rapidly absorbs water but it can stay on top of the VC-RGO coated part for many hours.



**Supplementary Figure 5.** PVA-GO composites films exhibit barrier properties similar to those of GO laminates but with improved mechanical strength. **a** – Weight loss for a container filled with water or other liquids and sealed with a 1  $\mu\text{m}$  thick PVA-GO membrane before and after its reduction with HI acid. The measurements were carried out at room temperature in a glove box. The green curve shows water permeation after the reduction in HI; the other curves are for non-reduced PVA-GO. **b** – X-ray diffraction for HI-reduced PVA-GO membrane. Inset: Photograph of a 2 cm $\times$ 2 cm steel plate coated with VC-reduced PVA-GO.

## **Supplementary Note 1. Comparison of RGO barrier films produced by various reduction methods**

There exists a large amount of literature on reduction of GO using different techniques, which is mainly focused on individual flakes and on improving their electronic properties<sup>1</sup>. Multilayer RGO and, especially, their barrier properties are much less explored, probably because most of the reduction techniques lead to severe structural damage and the material becomes extremely fragile after reduction, sometime turning into a powder. As an example, Supplementary Fig. 1 (left inset) shows an optical photograph of a thermally reduced GO membrane. It has a rough dull surface with numerous bubbles. This happens because, during thermal reduction, oxygen containing functional groups remove carbon atoms from the graphene lattice, which leads to release of gases such as CO and CO<sub>2</sub>. The gases accumulate into bubbles and result in the destruction of the fine layered structure of RGO laminates<sup>1</sup>. Poor quality of thermally reduced membranes is obvious from their dull appearance as compared with shiny smooth surfaces of RGO membranes reported in the main text (see Fig. 1).

Apart from thermal reduction, many chemical reducing agents such as hydrazine, sodium borohydride, etc. have been investigated<sup>1</sup>. Similar to thermally-reduced GO, most of the chemical reduction methods result in structural defects in the graphene lattice or destruction of the laminar structure due to release of gases. The right inset in Supplementary Fig. 1 illustrates such damages by showing a result of immersing a micron-thick GO membrane in a 50% hydrazine hydrate solution. During the vigorous reduction process, the GO membrane was completely destroyed. Similar damages to GO laminates were reported for reduction in sodium borohydride<sup>2</sup>. Nonetheless, one can significantly reduce such damages by slowing chemical reactions. To this end, we have used hydrazine vapors, which allowed us to obtain thin RGO films without visible damage. Supplementary Fig. 1 shows permeation properties of a 100 nm thick hydrazine-vapor-reduced GO coating on PET. As compared to HI-RGO of the same thickness, the former films are two orders of magnitude more transparent to He, which indicates more structural damage, even in this case of slow reduction and ultra-thin films. The principal reason for superior barrier properties of HI-RGO is that, during the reduction process in HI, most of oxygen-containing functional groups are released as H<sub>2</sub>O with little damage to the graphene lattice itself<sup>1</sup>. In turn, the released water is highly mobile within graphene capillaries<sup>3,4</sup>, which allows GO laminates to maintain their layered structure that becomes close to that of graphite after the reduction.

To further emphasize the uniqueness of the discussed HI- and VC- RGO barrier films, we have tested barrier properties of membranes made from RGO (essentially graphene) using its dispersions in organic solvents such as dimethylformamide (DMF) and N-methylpyrrolidone (NMP). These dispersions were prepared by sonication of bulk RGO followed by centrifugation<sup>5,6</sup>. The final graphene coatings and membranes were obtained from these solutions using the procedures described in the main text. Such films were found to be poor barriers with respect to all tested gases and vapors including helium, hydrogen, water and propanol. This is attributed to the lack of the laminar structure that is an important feature of films produced from GO solutions. RGO solutions do not form such fine layered structures. It is a specific interaction between functional groups on GO flakes, which leads to self-assembly into fine laminates. In contrast, graphene or RGO crystals form a non-interlocked

structure with high porosity, which allows easy permeation of gases. This indicates that the fine laminar structure is more important for superior barrier properties than the simple absence of defects in graphene sheets.

### **Supplementary Note 2. Effect of mechanical deformation and wear on barrier properties**

Mechanical robustness of barrier films is important for their practical applications. For qualitative assessment of mechanical stability of our RGO films, we have performed He tests for HI-RGO on PET before and after multiple (>10) folding to a radius of less than 1 mm in different directions. Supplementary Fig. 3a shows an example of our results and compares them with those for the industry-standard films (Al on PET), which experienced the same deformations. The Al film exhibited a 2-3 fold increase in He permeation rates whereas HI-RGO of a similar thickness showed no discernable change. Only films with HI-RGO thickness of  $\geq 200$  nm exhibited increased He leaks (see Supplementary Fig. 3). In this case, the resulting permeation rate were >100 times above our detection limit but still remained significantly lower than the gas permeation through the standard aluminized PET, even before its deformation.

The increased gas permeation after multiple folding for the thicker RGO films can be attributed to their weaker adhesion to PET compared to that of thin coatings. To support this idea, we have performed simple scratching tests on both thin and thick RGO on PET and found that thin (< 50 nm) RGO coatings on PET were stable with respect to scratching by a PTFE or wooden sticks whereas thicker films exhibited scratching marks. We believe that, similar to the standard Al films used as gas barriers, the scratchability, adhesion and mechanical robustness could be significantly improved by encapsulating RGO with another thin PET or polymer film<sup>7,8</sup>.

For further evaluation of the effect of mechanical strain on permeation properties of our barrier films, we have applied an isotropic strain by introducing a differential pressure across PET membranes. The maximum pressure we could apply to our PET films before rupturing them was approximately 4 bars and, therefore, we limited the pressure applied to the barrier films to 2 bars. Membranes were kept under this pressure for 30 minutes and permeation experiments were performed after releasing it. Supplementary Fig. 3b shows the effect of the strain on bare PET and on PET coated with Al and HI-RGO. Bare PET exhibits high He permeation but it changes little before and after applying the strain. The industry-standard aluminized PET became ten times more transparent to He after straining, nearly as transparent as bare PET. This shows that the strain test effectively destroyed the Al film as a gas barrier. Although we have also observed a tenfold increase in He permeation for strained HI-RGO on PET, the permeability remained much lower than for aluminized PET sheets before their straining (Supplementary Fig. 3).

Further studies and more rigorous tests are needed to understand the effect of mechanical deformation and wear on barrier properties of RGO but our qualitative experiments already indicate their superiority with respect to conventional barrier films.

### **Supplementary Note 3. RGO coating on rough and porous surfaces**

To understand the effect of surface roughness and porosity on barrier properties of our RGO films, we have deposited GO onto various surfaces. Those included polymer materials such as porous polycarbonate, polyvinylidene fluoride, polysulfone, etc. and extremely rough substrates such as brick and concrete surfaces. GO laminates on all these substrates were reduced by treating them with a VC solution at 80<sup>0</sup>C for 2 hours or 50<sup>0</sup>C for 24 hours. We have found that, although the barrier quality can be sensitive to roughness and porosity, GO laminates provide a high permeation barrier for all tested surfaces. As an example, Supplementary Fig. 4 shows a photograph of a conventional red brick that is half coated with VC-RGO. If water is poured on the brick, it stays only on the part covered with hydrophobic RGO. One can quantify the barrier properties of VC-RGO by measuring the time required for disappearance of the water puddle (Supplementary Fig. 4). The brick without coating absorbs water within a few seconds. In contrast, water on top of the RGO coated part stays for many hours and eventually disappears mainly due to evaporation. Taking the evaporation into account, we estimate that VC-RGO treated bricks are ~4,000 times more water repellant than uncoated bricks.

### **Supplementary Note 4. Polyvinyl alcohol modified GO for improved adhesion**

Adhesion between treated surfaces and RGO is critical for the perspective use of such films as chemical and anticorrosion coatings. Adhesion of RGO to plastic and glass surfaces has been found strong. Qualitatively, the graphitic films were more robust than the standard barrier films (Al on PET) as discussed above, although the wear properties require further quantification. In contrast, adhesion of RGO to metal surfaces was weak, which resulted in easy scratching and partial peeling of the protective coating. To overcome the drawbacks of weak adhesion to metal surfaces, we have employed the previous observation<sup>9-11</sup> that mechanical, electrical and biocompatible properties of GO laminates can be improved by interlayer cross-linking with PVA or other polymer molecules. For the purpose of this report, we have tested permeation properties of PVA-GO composite films, both before and after their chemical reduction.

PVA-GO samples were prepared by blending water solutions of GO and PVA by using a magnetic stirrer. The concentrations were chosen such that we achieved 60-80 weight percentage of GO in the final laminates, after evaporation of water. All the tested PVA-GO films exhibited similar properties, irrespective of their PVA fraction. We used vacuum filtration, drop casting and rod coating techniques to produce free standing PVA-GO membranes and PVA-GO films on substrates. Supplementary Fig. 5a shows examples of our permeation measurements for water and other organic vapors through a 1 $\mu$ m thick PVA-GO membrane, before and after its reduction with HI. Similar to GO, PVA-GO membranes completely block all gases and vapors except for water. After reduction of PVA-GO with HI, water permeation has reduced by four orders of magnitude (Supplementary Fig. 5).

We have also studied salt permeation properties of such cross-linked GO membranes and found that permeation rates are beyond our detection limit, too. We have tested not only HI- but also VC- reduced PVA-GO and observed no major differences. The inset of Supplementary Fig. 5b shows an optical photograph of a steel plate coated with VC-reduced PVA-RGO. Such protecting coatings exhibit good adhesion to metal surfaces including

copper, steel, nickel, etc. Copper foils coated with VC-reduced PVA-RGO were tested for acid corrosion. We could not detect any sign of corrosion in tests similar to those described in the main text and involving oxidized Si wafers protected with unmodified RGO (Fig. 3a of the main text).

Supplementary Fig. 5b shows X-ray diffraction for HI-reduced PVA-RGO membranes. They exhibit a layered structure similar to HI-RGO but with an interlayer separation of  $\approx 4.2$  Å, that is, considerably larger than in the membranes without PVA (see Fig. 3b of the main text). This increase in the interlayer distance is attributed to the presence of PVA molecules between reduced GO sheets (intercalation-like composites). Although the interlayer distance increases, the presence of polymer molecules trapped between the graphene sheets effectively blocks all molecular and ionic permeation through the extra space of 0.6 Å in the composite membranes.

We have also checked water solubility and swelling behavior of PVA-GO membranes by immersing them in water for 24 hours and then sonicating for 5-10 minutes. It is found that the composite membranes are highly stable and don't break even during the sonication, in agreement with the previous studies<sup>9</sup>. This enhanced stability can be due to the effect of hydrogen-like bonding between PVA molecules and GO sheets. Let us also note that PVA is one of many potential cross-linking agents<sup>12</sup> to make stronger and better barrier coatings with GO. We have performed similar experiments by using imidazole as a cross-linker and found performance similar to that of PVA cross-linked GO.

### **Supplementary References**

- 1 Chua, C. K. & Pumera, M. Chemical reduction of graphene oxide: a synthetic chemistry viewpoint. *Chem. Soc. Rev.* **43**, 291-312 (2014).
- 2 Pei, S. & Cheng, H.-M. The reduction of graphene oxide. *Carbon* **50**, 3210-3228 (2012).
- 3 Nair, R. R., Wu, H. A., Jayaram, P. N., Grigorieva, I. V. & Geim, A. K. Unimpeded permeation of water through helium-leak-tight graphene-based membranes. *Science* **335**, 442-444 (2012).
- 4 Joshi, R. K. et al. Precise and Ultrafast molecular sieving through graphene oxide membranes. *Science* **343**, 752-754 (2014).
- 5 Park, S. & Ruoff, R. S. Chemical methods for the production of graphenes. *Nature Nanotech.* **4**, 217- 224 (2010).
- 6 Hernandez, Y. et.al. High-yield production of graphene by liquid-phase exfoliation of graphite. *Nature Nanotech.* **3**, 563-568 (2008).
- 7 Tan, C. et al. Mechanical and environmental stability of polymer thin-film-coated graphene. *ACS Nano* **6**, 2096-2103 (2012).
- 8 Mueller, K., Schoenweitz, C & Langowski, H. C. Thin Laminate Films for Barrier Packaging Application – Influence of down gauging and substrate surface properties on the permeation properties. *Packaging Tech. Sci.* **25**, 137-148 (2012).
- 9 Li, Y.-Q., Yu, T., Yang, T.-Y., Zheng, L.-X. & Liao, K. Bio-Inspired Nacre-like Composite Films Based on Graphene with Superior Mechanical, Electrical, and Biocompatible Properties. *Adv. mater.* **24**, 3426-3431 (2012).
- 10 Tian, Y., Cao, Y., Wang, Y., Yang, W. & Feng, J. Realizing Ultrahigh Modulus and High Strength of Macroscopic Graphene Oxide Papers Through Crosslinking of Mussel-Inspired Polymers. *Adv. mater.* **25**, 2980-2983 (2013).



- 11 An, Z., Compton, O. C., Putz, K. W., Brinson, L. C. & Nguyen, S. T. Bio-Inspired Borate Cross-Linking in Ultra-Stiff Graphene Oxide Thin Films. *Adv. mater.* **23**, 3842-3846 (2011).
- 12 Hung, W. S. *et al.* Cross-linking with diamine monomers to prepare composite graphene oxide-framework membranes with varying d-spacing. *Chem. Mater.* **26**, 2983-2990 (2014).